Next Scientists
Journal of Social Sciences and Humanities Research Fundamentals

TYPE Original Research
PAGE NO. 84-92
DOI 10.55640/jsshrf-05-07-14



# Silver-doped Lithium-Boro-Carbonate Glass: Assessment of Structural and Thermoluminescence Features

Hayder. K. Obayes

Department of Physics Sciences, Faculty of Science Universiti Teknologi Malaysia,

Directorate General of Education in Babylon Governorate, Ministry of Education, Baghdad, 51001, Iraq

**OPEN ACCESS**

SUBMITED 31 May 2025
ACCEPTED 29 June 2025
PUBLISHED 31 July 2025
VOLUME Vol.05 Issue07 2025



**Abstract:** Three silver (Ag)-doped Lithium-Boro-Carbonate glass samples (hereafter named as LBAg0.2, LBAg0.4 and LBAg0.6) of molar composition 15Li2BO3-84.6H3CO3-xAg (x = 0.2, 0.4 and 0.6 mol%) were prepared by melt-quenching approach and characterized. Results displayed some appreciable changes in the thermoluminescence (TL), thermal and structural behaviors of the glasses due to Ag doping at various levels. Thermally durable (Hurby parameter ~ 0.5) and optically transparent glasses were achieved. XRD and FESEM analyses of the quenched samples verified their corresponding disordered nature and homogeneous morphologies. Three characteristic peaks related to the trigonal and tetrahedral stretching vibration modes of BO3 and BO4 units around 700.55-930.68 and 1072.07 cm-1 were observed in the FTIR spectra, accompanying by the peak shift with increasing Ag contents. DTA results showed the melting, crystallization, and glass transition peak at 700, 500 and 495 0C, respectively. TL measurement of the glasses under Co-60 gamma irradiation exhibited a single intense peak with the highest value of 194°C. LBAg0.4 glass at 50 Gy ⍰⍰-ray exposure revealed the maximum TL response and best linearity. The proposed glass system may be valuable for the development of radiation dosimeters.

**Keywords:** TL, Doping, Silver, Glass, and Kinetic parameters.

**Highlights**

- Three Ag-doped Lithium-Boro-Carbonate glasses were made and characterized.
- Overall properties of glasses were improved due to Ag doping.
- TL glow carve of glasses showed a peak around 192 °C.
- TL peak intensity and kinetic parameters was altered with the Ag contents variation in glasses.
- Obtained glasses revealed excellent sensitivity and linearity over the entire dose range.
- Achieved best glass composition may be potential for radiation dosimeters.

**Graphical abstract**

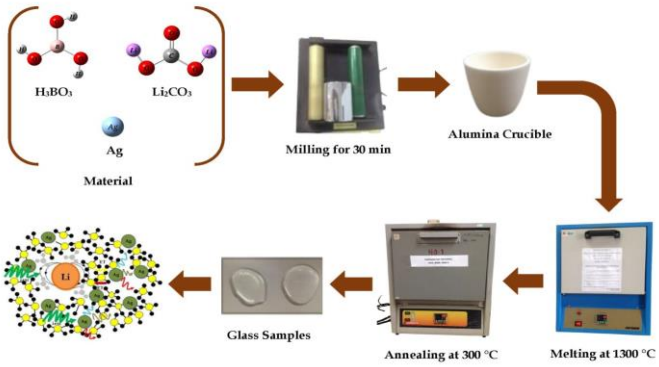


**INTRODUCTION:** Because of the impurity/dopant presence in the materials composition, diverse natural and synthetic borate systems are usually refined by special chemical agents. They find several practical commercial applications such as radiation dosimeters. Meanwhile, a good understanding regarding the complex crystal structure and physicochemical properties of borate systems became essential. For widespread technological uses various types of borates with unique behavior were mixed to get emergent features [1, 2]. Categorically, lithium borates were obtained by mixing lithium carbonate (Li2CO3) with hydroborate (H3BO3) both in powder form at stoichiometric ratios followed by melting at 750 °C for 14 h [3, 4]. To improve the TL characteristics of lithium borate-based glass systems lithium tetra-borate and lithium tri-borate glasses were formulated [5, 6]. Powders of lithium borate (white in color and odorless) melts at 917 °C with the density and solubility range of 2.4 g/cm³ and 1-10%, respectively [7]. It also shows strong piezoelectric characteristics [8]. In comparison to lithium tetraborate glass system, lithium borate glasses are attractive due to their extraordinary network structure, physical and TL traits useful for high-performance dosimeter development [9]. Particularly, lithium borate glass-based TL dosimetry became a significant tool for quantifying the ionizing radiation exposures [10], which is mainly due to their closeness of atomic number to living tissue. Lately, LiB3O5-based glass system became attractive in the medical field due to their prospective TL properties.

Different rare earth elements and metallic particles-doped lithium borate glasses were synthesized and irradiated at various ionizing doses to determine their TL glow curves. Various borate-based advanced reagents like hydrous and anhydrous boric acid, anhydrous and pentahydrate borax, and sodium perborate were intensively studied to examine their recrystallization behavior [11]. Borate systems made at stoichiometric composition possess distinct crystal structures and chemical characteristics, finding their diverse technological uses [12,13]. Some bi-products of lithium borate glass systems such as lithium tri-borate and tetra-borate show excellent TL and piezoelectric response at wide dose range [14, 15, 16], enabling them advantageous for TL dosimetry [17].

Based on these facts, three Ag-doped Lithium-Boro-Carbonate glasses of molar composition 15Li2BO3-84.6H3CO3-xAg (where x = 0.2, 0.4 and 0.6 mol%; glass codes: LBAg0.2, LBAg0.4 and LBAg0.6) were prepared using melt-quenching method and characterized in detail. The morphologies, structures and TL characteristics of the obtained glasses were evaluated as a function of Ag contents. The results showed an overall improvement in the glass properties due to Ag doping. The TL glow carve of the glasses showed a prominent peak at 192 °C, with alteration in the TL peak intensity and kinetic parameters due to increasing Ag contents. In addition, these glasses exhibited outstanding sensitivity and linearity over the entire dose range. The glass sample made with 0.4 mol% of Ag showed the optimum TL properties, thus nominated for radiation dosimeters construction and medical applications. The results obtained were compared with state-of-the-art dosimeters made from gold-doped lithium-borate glasses.

**Glass synthesis and characterizations**

An electric furnace was used to make all glasses. Pure powders of Li2BO3, H3CO3 and Ag were ground, mixed uniformly and placed in the alumina crucible followed by melting at 1300°C for 1 h inside the furnace. Once the mix composition was melted entirely, the molten fluid was transferred onto a pre-heated steel plate followed by rapid cooling. Next, the frozen solid was subjected to annealing for 3 h at 300 °C, achieving the glass samples. The obtained glasses were subjected to heating for further stabilization followed by slow cooling inside the furnace at an ambient temperature to evade any thermal strain that can cause glass cracks.

The resultant samples were analyzed using XRD (D5000 Siemens Diffractometer), FESEM, DTA, FTIR and optical emission measurements. The TL behaviors of the glasses were examined under the dose exposure of 50 Gy γ-ray photons from a Co-60 radiation source. The glow curves of the glasses were obtained from the TL profiles. Table 1 displays the composition and codes of all the produced glass samples.

**Table 1: Glass compositions and names**

| Glasses | $Li_2CO_3$ (mol%) | $H_3BO_3$ (mol%) | Ag (mol%) |
|---|---|---|---|
| LBAg0.2 | 15 | 84.8 | 0.2 |
| LBAg0.4 | 15 | 84.6 | 0.4 |
| LBAg0.6 | 15 | 84.2 | 0.6 |

## Results and discussion

### 3.1 Glass structure and morphology

Figure 1 displays the room temperature powder XRD profiles of all samples. The XRD patterns of all samples without any intense Bragg peak (no crystallinity) and with a broad hunch clearly indicated their true amorphous phases. The XRD measurements were performed at the scan rate of 0.05 degrees/s. [18].

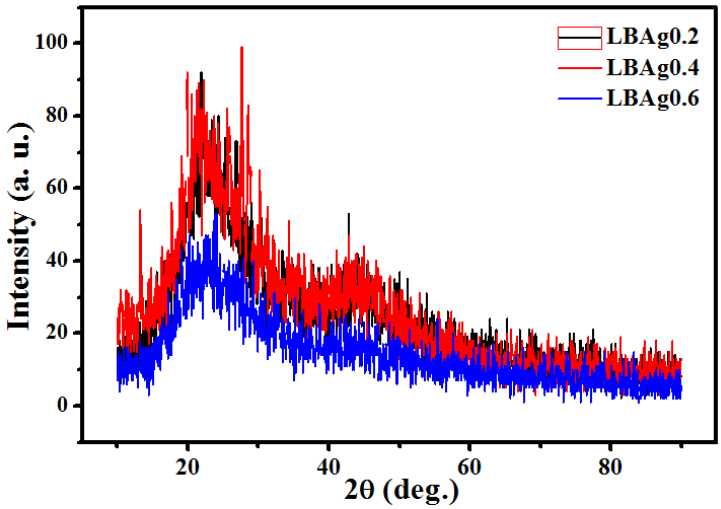


**Figure 1: XRD profiles of the samples.**

Figure 2 illustrates FESEM micrographs of all three samples, displaying their uniform surface microstructures in the absence of any visible grains or crystallites [1]. These results reconfirmed the disordered and transparent character of the quenched samples.

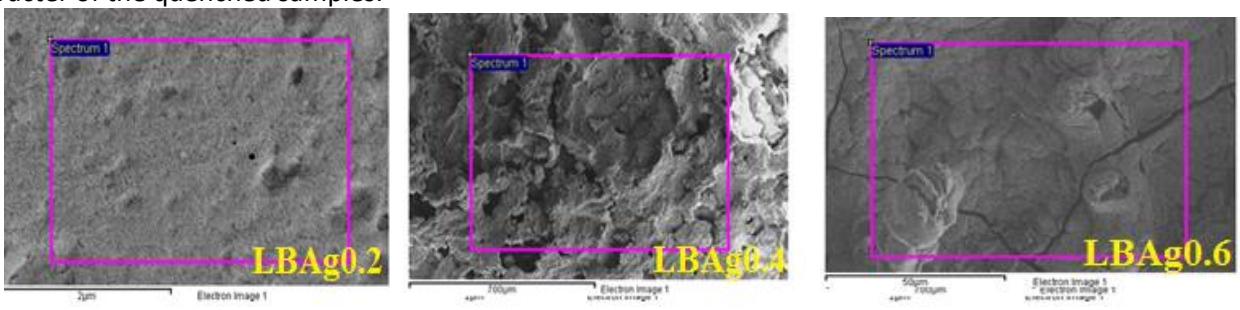


**Figure 2: FESEM micrographs of the prepared glasses**

Figure 3 displays the FTIR spectra of all glasses, exhibiting 3 fundamental bands with peaks at 700.58-918.63 and 1064.45 cm-1 which were ascribed to the stretching vibration modes of trigonal and tetrahedral units. With increasing Ag contents, the peaks showed a shift towards lower wavenumber, which was mainly because of higher atomic weight of silver compared to the atomic weights of other glass constituents. This observation was in good agreement with other reports [3-5]. The observed band at 700.58, 706.08 and 700.54 cm-1 were due to the bending vibration modes of B-O-B linkage and stretching vibration modes of BO3 and BO4 units in the glass network structure [6, 7]. The IR bands appeared in the region of 918.63-985.35 cm-1

and 1064.45-1049.37 cm-1 were due to stretching vibration modes of B-O linkages associated with the BO4 units [8-10]. The strong bonding of tetrahedral BO4 units compared to the triangular BO3 units lead to more compact network structure and thus higher glass density [11]. The symmetric stretching vibration modes of B-O linkages in BO3 units produced the intense IR peak at 1200-1500 cm-1 [12, 13]. The peak absorption intensities of all bands were lowered with the increase of Ag contents in the glass matrix. The symmetric stretching vibration modes of O-H group in water (H-O-H) produced the broad IR band around 3400-4000 cm–1 [14, 15]. Table 3 shows the FTIR analysis results.

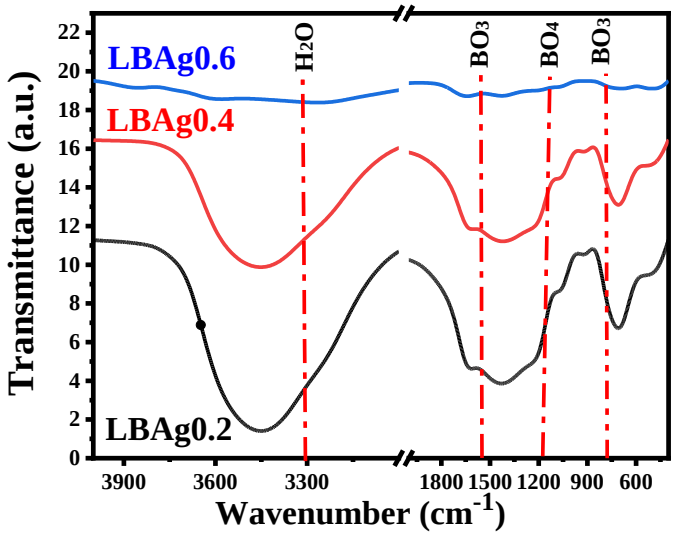


**Figure 3: FTIR spectrum of glasses.**

**Table 2: FTIR bands assignment and location.**

| Glasses | Band assignment ($cm^{-1}$) | | | | | |
|---|---|---|---|---|---|---|
| | B-O (Trigonal $BO_3$ units stretches) ± 0.06 | | B-O (tetrahedral $BO_4$ units stretches) ± 0.07 | | O-H (in $H_2O$) ± 0.01 | Stretching vibration ±0.03 |
| LBAg0.2 | 1228.05 | 1428.13 | 918.63 | 1064.45 | 3449.24 | 700.58 |
| LBAg0.4 | 1219.21 | 1410.43 | 927.57 | 1067.20 | 3445.58 | 706.08 |
| LBAg0.6 | 1204.03 | 1440.69 | 985.35 | 1040.37 | 3447.77 | 700.58 |

### 3.2 Thermal features of samples

The DTA data of the samples produced provided the values of temperatures related to the melting ($T_m$), sublimation ($T_s$), crystallization ($T_c$) and glass transition ($T_g$). Kauzmann equation of used to obtain the glass forming capacity of the proposed mix composition:

$$\mathrm{Trg} = \frac{T_g}{T_m} \quad (1)$$

According to the Kauzmann criteria, if 0.5 ≤ Trg ≤ 0.66 then the glass forming ability is considered as satisfactory. These glasses satisfied the Kauzmann condition.

Hurby criteria can also be used to determine the thermal of the glasses:

$$\mathrm{Hg} = \frac{T_c - T_g}{T_m - T_c} \quad (2)$$

If Hg ≤ 0.1 the glass is said to be unstable and if Hg ~ 0.5 it is considered as highly stable [2]. The calculated values of Trg and Hg for all synthesized glasses are presented in Table 3.

**Table 3: Thermal characteristics of all glass samples.**

| Glasses | Mg (mol%) | *Tg* (°C) | *Tc* (°C) | *Tm* (°C) | *Trg* | *Hg* | *Tc-Tg* (°C) |
|---|---|---|---|---|---|---|---|
| LBAg0.2 | 0.03 | 495.93 | 655.02 | 761.71 | 0.65 | 1.49 | 159.09 |
| LBAg0.4 | 0.05 | 496.17 | 658.74 | 763.94 | 0.64 | 1.54 | 162.57 |
| LBAg0.6 | 0.07 | 497.88 | 645.29 | 770.54 | 0.64 | 1.17 | 147.41 |

Figure 4 shows the DTA results of LBAg0.2, LBAg0.4 and LBAg0.6 samples which exhibited endothermic peaks of Tg correspondingly at 495.93, 496.17 and 497.88 °C. The Tc and Tm peaks for LBAg0.2, LBAg0.4 and LBAg0.6 samples appeared correspondingly at 655, 658 and 645 °C; and at 761, 763 and 770 °C. Trg and Hg values for LBAg0.2, LBAg0.4 and LBAg0.6 samples were correspondingly 0.65, 0.64 and 0.64 and 1.49, 1.54, and 1.71, indicating the attainment of good quality and thermally durable glasses.

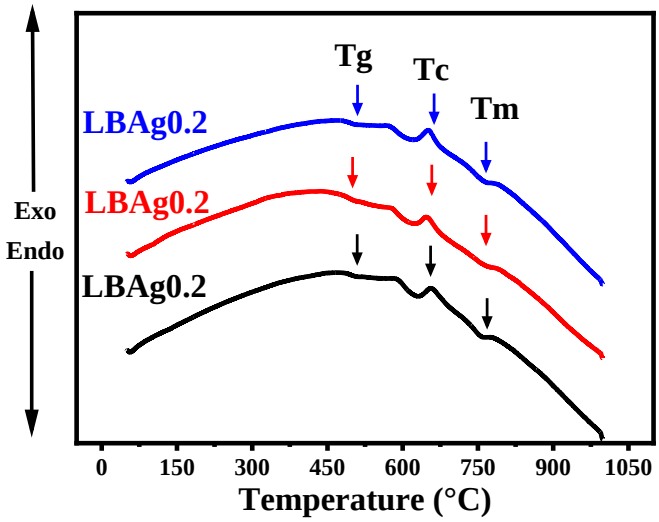


**Figure 4: DTA profiles of all the studied glasses.**

### 3.3 Optical emission spectrum of glasses

Figure 5 elucidates photoluminescence emission spectrum of all the glasses, wherein the peak intensity and position were gradually altered with the change of Ag doping concentration. The PL peaks of LBAg0.2, LBAg0.4 and LBAg0.6 samples occurred at 399.98, 393.53 and 397.89 nm, respectively. Irrespective of Ag contents, the intensity of all PL peaks was enhanced accompanied by an abrupt shift towards lower frequency. In addition, the PL peak intensity could drop accompanied by a shift toward higher frequency at Ag contents of 0.6 mol%. The absorbed change in the PL peak profiles can be ascribed to the formation of new chemical complex in the glass network due to the inclusion of reactive silver [16].

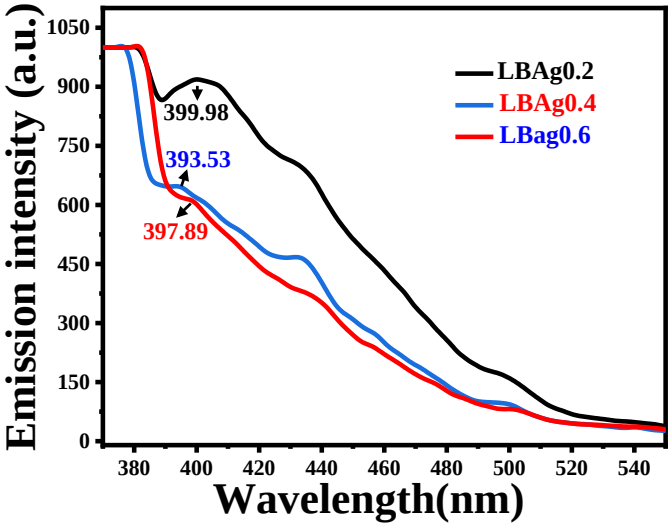


**Figure 5: PL emission spectrum of glasses.**

### 3.4 TL properties of glasses

Figure 6 shows the TL glow curves of the synthesized glasses under the exposure of 50 Gy dose of Co-60 gamma irradiation, displaying a prominent peak at ~192 °C with intensity variation depending on Ag doping levels. The observed variation of the TL glow profiles was mainly due to the radiation-assisted recombination of the excited electrons at the defect-filled valence band in the glass, yielding an increase in the TL intensity [13].

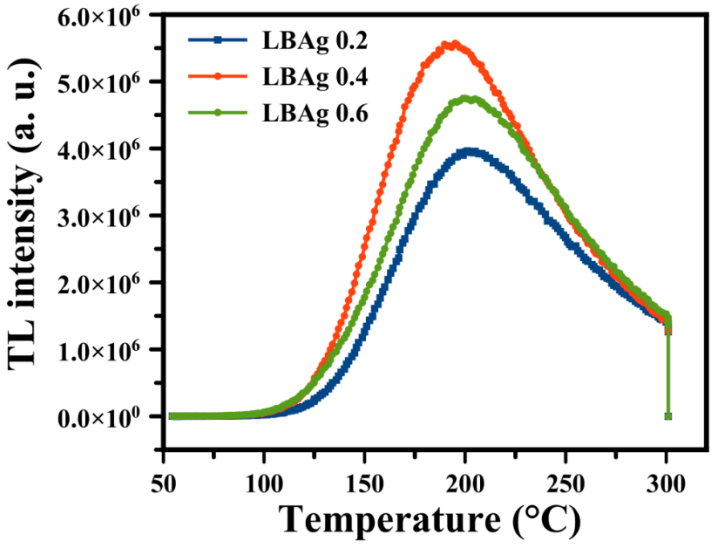


**Figure 6: TL glow curves of glasses.**

For efficient dosimeter fabrication, the material must show a linear relationship amid doses and TL response. In the current study, LBAg0.4 glass showed excellent linearity in the range of 10 to 50 Gy (Figure 7), indicating its advantages for radiation dosimeter fabrication.

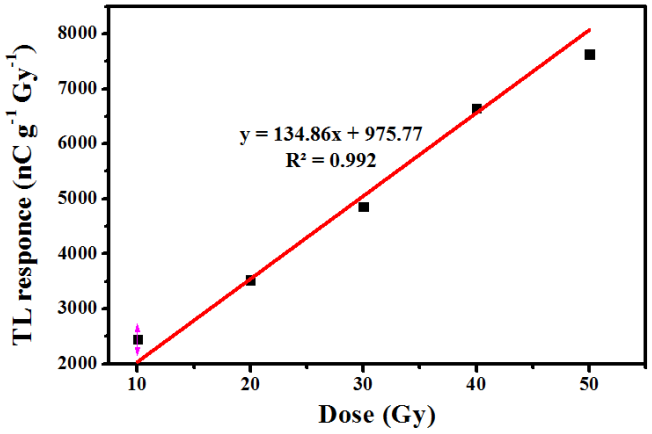


**Figure 7: Co-60 gamma irradiation dose-dependent TL response of LBAg0.4 sample.**

The TL sensitivity (nC $g^{-1}$ $Gy^{-1}$) of the proposed dosimeter was measured from the glow curve area related to the material's mass and dosage, indicating their excellent reactivity of the glasses with the radiation. The TL sensitivity was computed from the dose to sensitivity ratio (nc/m). LBAg0.4 glass exhibited a sensitivity of 134.86 µC $g^{-1}$ $Gy^{-1}$ under the exposure of Co-60 gamma irradiation dose range of 10-50 Gy. The overall pattern of the TL glow curve was strongly affected by the trap levels [20]. To further understand the behavior of the TL glow curves that determine the dosimetry potential of a material, multiple kinetic parameters were calculated, providing a mechanism of TL. These parameters include kinetic orders (b), geometric (µg) and frequency (s) factors, activation energies (E), and trap depths (E). The peak form of the glow curve and initial rising procedure were used to determine the values of s and E. The Chen approach called peak shape procedure was used to evaluate the kinetic parameters [21]. The values of temperatures for the glow curve peak (T_m), and T_1 and T_2 associated with the full width at half maximum were vital in determining the accurateness of the approach [22]. Figure 8 illustrates the TL glow curve of LBAg0.4 glass analyzed using the peak shape approach. The geometric factors were calculated via the relations:

$$\mu_g = \frac{T_2 - T_m}{T_2 - T_1} \quad (3)$$

and

$$\mu_g = \frac{T_2 - T_m}{T_m - T_1} \quad (4)$$

For the first order and second order kinetics, the ideal values of $\mu_g$ are 0.42 and 0.52, respectively. In addition, the kinetic order was evaluated using Balarin approach [23]:

$$b = 0.0365 \times 10^{2.95 \times \mu_g} \quad (5)$$

The value of b for LBAg0.4 glass was 2.14, indicating second kinetics. Following the earlier report [24], the activation energy was obtained via:

$$E = C_\alpha \frac{k_B T_m^2}{\alpha} - b_\alpha 2 k_B T_m \quad (6)$$

where $k_B$ is the Boltzmann constant, and α signifies the parameters τ, δ, and ω related to LBAg0.4 glass (Figure 8). The values of $C_\alpha$ and $b_\alpha$ were computed via:

$$C_\tau = 1.510 + 3.0(\mu_g - 0.42),\ b_\tau = 1.58 + 4.2(\mu_g - 0.42) \quad (7)$$

$$C_\delta = 0.976 + 7.3(\mu_g - 0.42),\ b_\delta = 0 \quad (8)$$

$$C_\omega = 2.52 + 10.2(\mu_g - 0.42),\ b_\omega = 1 \quad (9)$$

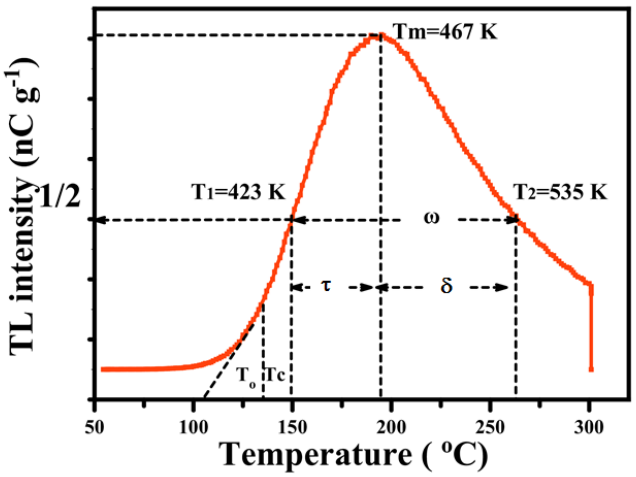


**Figure 8: TL glow curve of LBAg0.4 glass with the peak shape analysis.**

Table 4 displays the calculated values of C_α and b_α for LBAg0.4 glass, wherein α can be τ, δ, and ω.

**Table 4: The constants c and b for the LBAg0.4 glass samples.**

| Glass | Parameters | τ | δ | ω |
|---|---|---|---|---|
| LBAg0.4 | $C_\alpha$ | 2.05 | 2.29 | 4.35 |
| | $b_\alpha$ | 2.33 | 0 | 1 |

The value of s was evaluated via:

$$\frac{\beta E}{kT_m^2} = s\left[1 + (b-1)\frac{2kT_m}{E}\right]\exp\left(-\frac{E}{kT_m}\right) \qquad (10)$$

where β is the linear rate of heating rate.

Table 5 shows the values of activation energies (in eV) for LBAg0.4 glass. Herein, E_□ , E_(□ ) and 〖 E〗 _ω are activation energies corresponding to the first and second half width at the glow peak profile on the rising and falling sides, and overall glow profile width. A comparison of the calculated kinetic parameters at the adsorbed dose confirmed a constant energy distribution among the trap levels, wherein the deeper traps needed higher energy and temperature in liberating the electrons within the glass matrix [25]. Briefly, the dose detection performance of LBAg0.4 glass was understood from the obtained values of kinetic parameters, frequency factors and activation energies.

**Table 5: Significant kinetic parameters of LBAg0.4 glass.**

| Glass | Parameters | | | |
|---|---|---|---|---|
| | $E_\tau\,(eV)$ | $E_\delta(eV)$ | $E_\omega\,(eV)$ | Average |
| **LBAg0.4** | 0.688 | 0.632 | 0.345 | 0.655 |

## Conclusion

Three Lithium-Boro-Carbonate glasses with Ag doping were prepared by the melt quenching approach. Glasses were characterized to determine the Ag concentration dependent structural, morphological, thermal and TL attributes. XRD and FESEM analyses confirmed the glassy nature of samples. DTA results verified their stability. FTIR measurement confirmed the presence of functional chemical bonds of various structural units in the glass network, leading to compact structure, transparency and thermal durability. Silver activation in the glass network structure could create the luminescence centers by elevating from the valence band top to the nearby oxygen ions energy levels and novel electron traps, thus increasing the TL response. The glow curves of the glasses showed a single distinct peak at 194 °C with excellent kinetic parameters, signal reproducibility and linear dose response. It was asserted that the proposed glass composition can be beneficial to TL dosimetry for ionizing radiation measurement. It short, the overall properties of the LB glasses can be customized via controlled Ag doping.

## Acknowledgements

Financial support and IDF fellowship (UTM.J.10.01/13.14/1/128) are highly appreciated.

## References

1. Obayes, H.K., Thermoluminescence Properties of Strontium-Copper Co-Doping Lithium-Borate Glass For Ionizing Radiation Application. 2017, Universiti Teknologi Malaysia.
2. Alajerami, Y.S.M., Et Al., The Effect Of Titanium Oxide on The Optical Properties of Lithium Potassium Borate Glass. Journal of Molecular Structure, 2012. 1026: P. 159-167.
3. Pal Singh, G., Et Al., Investigation of Structural, Physical And Optical Properties of Ceo2Bi2O3B2O3 Glasses. Physica B: Condensed Matter, 2012. 407(21): P. 4168-4172.
4. Singh, G.P., Et Al., Density and FTIR Studies of Multiple Transition Metal Doped Borate Glass. Materials Physics and Mechanics, 2012. 14: P. 31-36.
5. Pal Singh, G. and D. Singh, Spectroscopic Study of Zno Doped Ceo2PboB2O3 Glasses. Physica B: Condensed Matter, 2011. 406(18): P. 3402-3405.
6. Pal Singh, G. And D. Singh, Modification In Structural and Optical Properties of Ceo2 Doped BaoB2 O3 Glasses. Journal Of Molecular Structure, 2012. 1012: P. 137-140.
7. Pisarski, W.A., J. Pisarska, And W. Ryba-Romanowski, Structural Role of Rare Earth Ions In Lead Borate Glasses Evidenced By Infrared Spectroscopy: BO3↔ BO4 Conversion. Journal of Molecular Structure, 2005. 744: P. 515-520.
8. Singh, G.P., Et Al., Modification In Structural And Optical Properties of Zno, Ceo2 Doped Al2O3 PboB2 O3 Glasses. Physica B: Condensed

Matter, 2012. 407(8): P. 1250-1255.

**9.** Juline, C., Et Al., Infrared Studies of The Structure of Borate Glass. Mater. Sci. Eng., B, 1989. 3: P. 307-312.

**10.** Gaafar, M., Et Al., Elastic Properties and Structural Studies on Some Zinc-Borate Glasses Derived From Ultrasonic, FT-IR And X-Ray Techniques. Journal Of Alloys And Compounds, 2009. 475(1): P. 535-542.

**11.** Singh, D., Et Al., Optical and Structural Properties of Li2OA2O3B2O3 Glasses Before And After Γ-Irradiation Effects. Journal Of Applied Physics, 2008. 104(10): P. 103515-103515-5.

**12.** Gandhi, Y., Et Al., Influence of WO3 on Some Physical Properties of MO2O3–B2O3 (M= Ca, Pb and Zn) Glass System. Journal of Alloys And Compounds, 2009. 485(1): P. 876-886.

**13.** Sharma, G., Et Al., Effects of Gamma Irradiation on Optical And Structural Properties of Pbo–Bi2O 3–B2O3 Glasses. Radiation Physics And Chemistry, 2006. 75(9): P. 959-966.

**14.** Husung, R.D. And R.H. Doremus, The Infrared Transmission Spectra of Four Silicate Glasses Before And After Exposure To Water. Journal of Materials Research, 1990. 5(10): P. 2209-2217.

**15.** Dunken, H. And R.H. Doremus, Short Time Reactions of a Na2O-Cao-Sio2 Glass With Water And Salt Solutions. Journal of Non-Crystalline Solids, 1987. 92(1): P. 61-72.

**16.** Liu, X., Et Al., Crystal And Solution Photoluminescence of Mag24 (SR) 18 (M= Ag/Pd/Pt/Au) Nanoclusters And Some Implications For The Photoluminescence Mechanisms. The Journal of Physical Chemistry C, 2017. 121(25): P. 13848-13853.